Available online at www.sciencedirect.com
SCIENCE DIRECT
Journal of Physics and Chemistry of Solids 66 (2005) 1838–1843
JOURNAL OF PHYSICS AND CHEMISTRY OF SOLIDS
www.elsevier.com/locate/jpcs

Cation order–disorder in $Pb(B^{II},B^{V})O_3$-related relaxors: The random-layer model investigated by Monte Carlo simulation

Hichem Dammak [a], Marc Hayoun [b,*]

[a] *Laboratoire Structures Propriétés et Modélisation des Solides, CNRS UMR 8580, École Centrale Paris, Grande voie des Vignes, F-92295 Châtenay-Malabry, France*

[b] *Laboratoire des Solides Irradiés, CEA/DSM, CNRS UMR 7642, École Polytechnique, F-91128 Palaiseau cedex, France*

Received 20 February 2004; accepted 28 September 2005

Abstract

The charge-balanced random-layer model for ordered lead-based perovskites $Pb(B^{II}_{1/3}B^{V}_{2/3})O_3$ was investigated by using the standard Metropolis Monte Carlo method on a rigid lattice with simple ionic model. Our results show that in the structure formula $Pb[B']_{1/2}[B'']_{1/2}O_3$, where all B″-sites are occupied by B^V cations, chemical order of B^{II} and B^V cations does exist in B′-sites and the ordered structure has an hexagonal symmetry. An order–disorder transition as a function of temperature is evidenced by an abrupt variation of both the heat capacity and a long-range order parameter. Finally, the evolution of the short-range order parameter versus temperature shows that a local order remains in B′-sites contrary to the charge-balanced random-layer model that suggests that B′-sites are randomly occupied. This local order could be helpful to clarify some experimental results.

PACS index categories: 07.05 Tp; 64.60.Cn; 65.40.Ba; 77.84.Dy

Keywords: A. Oxides; D. Crystal structure; D. Ferroelectricity; D. Phase transitions; D. Specific heat

1. Introduction

Lead based cubic perovskites, $PbB'_xB''_{1-x}O_3$, are attractive relaxor ferroelectrics because of their high dielectric constant which is frequency dependent and has a broad maximum as a function of the temperature [1,2]. It is known that dielectric properties may be strongly influenced by local order on the B-sites that is common in these relaxor ferroelectrics [3–5]. Thus, to improve the dielectric properties it is important to investigate the atomic structure of the long- and short-range order.

In the $Pb\,B^{III}_{1/2}B^{V}_{1/2}\,O_3$ compounds, like $PbSc_{1/2}Ta_{1/2}O_3$ (PST) [6,7] and $PbSc_{1/2}Nb_{1/2}O_3$ (PSN) [8], a 1:1 ordered structure is evidenced and corresponds to NaCl-type (Fm $\bar{3}m$) arrangement of cations B^{III} and B^V in the B-sites sublattice by doubling of the unit cell.

In the $Pb\,B^{II}_{1/3}B^{V}_{2/3}\,O_3$ compounds, like $PbMg_{1/3}Nb_{2/3}O_3$ (PMN) [9,10] and $PbZn_{1/3}Nb_{2/3}O_3$ (PZN) [11], diffraction studies have revealed ordered domains which present {1/2 1/2 1/2} superlattice reflections. Two models have been proposed for these ordered structures: the space-charge model and the charge balanced random-layer model [12–16]. In the space-charge model, it is postulated that the two different B-sites, called B′ and B″, in the 1:1 ordered structure are occupied exclusively by the B^{II} and B^V cations, respectively, in the form $Pb[B^{II}]_{1/2}[B^V]_{1/2}O_3$. Consequently, these ordered regions carry a net negative charge. For overall electroneutrality, an equal and oppositely charged, disordered, B^V rich matrix is proposed. An alternative model has been proposed for this material, the charge balanced random-layer model (RL). Here, the B″-sites are exclusively occupied by B^V, whereas the B′-sites contain a random distribution of B^{II} and remaining B^V. The structural formula can be represented as $Pb[B^{II}_{2/3}B^{V}_{1/3}]_{1/2}[B^V]_{1/2}O_3$ using a face centred (Fm $\bar{3}m$) superstructure. In this case, the ordered domains are microscopically charge balanced. This model has then been confirmed by Yan et al. [15] on the basis of high-resolution Z-contrast imaging of ordered domains in PMN.

The RL model has been used extensively to describe the ordered structures observed in several lead based complexes perovskites such as, La-doped PMN or PZN [11], PMN-PMT, PMT-PST [16], PMT-PZ [17] and PMN-PSN [18] solid solutions. Dmowski et al. [17] show that annealing of

* Corresponding Author. Fax: +33 0 1 6933 3022.
E-mail address: marc.hayoun@polytechnique.fr (M. Hayoun).

0022-3697/$ - see front matter © 2005 Elsevier Ltd. All rights reserved.
doi:10.1016/j.jpcs.2005.09.071

$Pb(Mg_{0.3}Ta_{0.6}Zr_{0.1})O_3$ (PMT-10%PZ) ceramic solid solution at ~1600 K produced significant increases in the volume fraction of the ordered phase (>95%) and the size of the chemically ordered regions (~100 nm). On the basis of X-ray Rietveld refinement, authors show that ordered regions are well described by the Fm $\bar{3}m$ superstructure $Pb[Mg_{0.6}Ta_{0.2}Zr_{0.2}]_{1/2}[Ta]_{1/2}O_3$ with the B′-site randomly populated by Mg, Zr and remaining Ta cations.

However, for the following it is important to note that for these compounds in which Pb cations were substituted by Ba cations ($BaB^{II}_{1/3}B^{V}_{2/3}O_3$) ordered phases have hexagonal symmetry where B^{II} and B^{V} cations occupy successive (111) cubic planes in the sequence B^{II}–B^{V}–B^{V}. For example, the 1:2 ordered structure was observed in BMN [19], BZT [20] and BMT [21].

Electrostatic energy calculations were first performed by Bursill et al. [14] on some possible ordered structures in PMN. The authors showed that the space-charge model (1:1 order) gives, as expected, a higher energy than the 1:2 ordered structure along [111] which is usually observed in barium based perovskites.

Later, by using Monte Carlo calculations and pure Coulomb interactions to study the disorder on B-sites, Bellaiche et al. [22] showed that the 1:2 order is the most stable. Moreover, a partial substitution of B^{II} and B^{V} by B^{IV} (giving $Pb[B^{II}_{1/3}B^{V}_{2/3}]_{1-x}[B^{IV}]_xO_3$) with a rate of 5 to 25% leads to the order described by the RL model. In this case, the B″ sublattice is almost entirely occupied by B^{V} whereas the B′ sublattice is composed of B^{II}, B^{IV} and the remaining B^{V} cations.

In this paper, we shall analyse the possible order of B^{II} and B^{V} cations in the B′-sites inside the $Pb[B^{II}_{2/3}B^{V}_{1/3}]_{1/2}[B^{V}]_{1/2}O_3$ structure as a function of the temperature, by rigid-lattice Monte Carlo sampling. The order–disorder transition is characterised by using short-range and long-range order parameters.

2. Computational details

The interactions between ions of the studied system, $Pb[B^{II}_{2/3}B^{V}_{1/3}]_{1/2}[B^{V}]_{1/2}O_3$, are modelled by the coulombic terms. Since the real ion charges are unknown in this structure and their determination needs a full ab initio study, we have used the nominal charges for this preliminary study. Non-coulombic terms, both repulsive and attractive ones, have been ignored. Thus, this model is simple but note that the coulombic contribution represents almost the total energy [23]. As usual, the Ewald method [24] has been used to calculate the Coulomb terms. The Madelung energy corresponds to electrostatic energy normalised by $-e^2/a$ where a is the lattice parameter of the unit cell. The Madelung energy calculated for the $AB^{IV}O_3$ structure (CMI), and for the well known 1:2 ordered structure along [111] (HexM) are equal to 49.5098 and 50.9876, respectively and they are close to those calculated by Bursill et al. [14] (Table 1).

The chemical disorder on the B′ sublattice has been investigated by using the standard Metropolis Monte Carlo on a rigid lattice. The system consists on a box of 6×6×6 cells of 5 atoms (1080) corresponding to 108 B′-sites on which exchanges are operated between B^{II} and B^{V} atoms. Periodic boundary conditions have been employed. A typical equilibrium run corresponds to a total number of exchange attempts per site of 50,000. Systems of 12×12×12 and 18×18×18 cells have also been used to test the size effects (see Section 4.4).

3. B′ sub-lattice ordered structures

We initially calculated the Madelung energy for the disordered RL structure by averaging the calculated values for all possible configurations. This means that the B′ sub-lattice is randomly disordered. The Madelung energy is equal to 50.6136 and is higher than that of the space charge structure (50.5328) showing that the RL structure is more stable than the space-charge structure.

The RL model suggests that atoms are randomly distributed in the B′ sub-lattice. Nevertheless, no investigation has been carried out on such a disorder. Therefore, we tried to build an ordered structure by considering the stacking of the (111) planes and especially the distribution of the B^{II} and B^{V} ions in the B′ sub-lattice. Taking into account the stacking sequence of all the (111) planes (ABC…) and the alternation of the B′ and B″ planes, a periodicity of six planes is imposed and the overall stacking sequence is $A_1B_2C_1A_2B_1C_2$… (Fig. 1(a)). B_2, A_2 and C_2 planes contain B^{V} ions (B″ sub-lattice) whereas A_1, C_1 and B_1 contain B^{II} and B^{V} ions (B′ sub-lattice). For instance, in the A_1 plane, ions are ordered as shown in Fig. 1(b) and then the C_1 and B_1 planes are obtained by applying a translation of $a/3$ [114] and $2a/3$ [114], respectively (Fig. 1(c)). This ordered structure is called RLII and its Madelung energy is higher than that of the disordered RL structure (Table 1).

Table 1
Madelung constant and short-range order parameters, α_1 and α_2

	Structure name	Symmetry	Madelung this work	Madelung Ref. [14]	α_1	α_2
$AB^{IV}O_3$	CMI	Cub.	49.5098	49.5098	–	–
Space charge model (1:1 order)	CMII	Cub.	50.5328	50.5326[a]	–	–
Randomly disordered B′	RL	Cub.	50.6136	–	0	0
	RLI	–	50.9213	–	−1/4	1/6
Ordered B′	RLII	Orth.	50.9288	–	−1/4	0
	RLIII	Hex.	50.9288	–	−1/4	0
1:2 order	HexM	Hex.	50.9876	50.9877	–	–

[a] We corrected the erroneous value of 50.3326 given in Table 2 of Ref. [14].

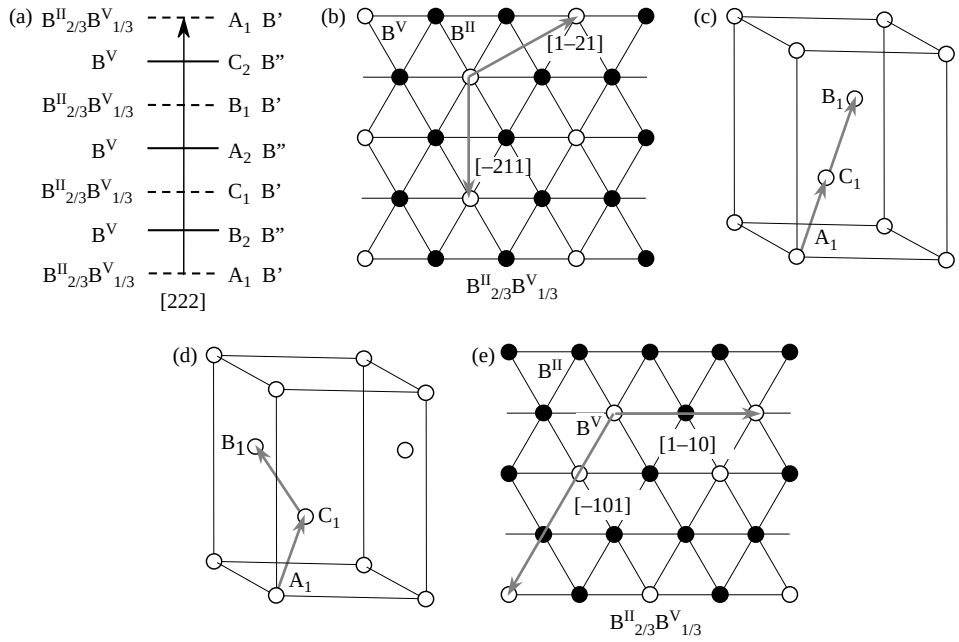

Fig. 1. Long-range order in the RL structures. (a) Stacking sequence of B′ and B″ (111) planes. (b) Order of B^{II} and B^{V} cations in the (111) B′ plane in the RLII and RLIII structures. (c) and (d) 3D stacking sequence of B′ (111) planes in RLII and RLIII, respectively. (e) Order of B^{II} and B^{V} cations in the (111) B′ plane in the RLI structure.

On the other hand, we tried to obtain an ordered structure by using the Metropolis Monte Carlo simulations. Calculations were performed at high temperature and then the structure is followed during a very slow decrease of the temperature. Two ordered structures were obtained (Fig. 2), RLI for which the Madelung energy lies between that of the disordered RL and RLII (Table 1), and RLIII which has exactly the same Madelung energy as RLII. The RLIII structure is similar with that of RLII and only differs by the stacking of the A_1, C_1 and B_1 planes (Fig. 1(d)). The symmetry of the RLIII structure is hexagonal whereas the symmetry of the RLII structure is orthorhombic. The structure of RLI is based on the stacking of B′ (111) planes in which B^{II} and B^{V} cations are distributed as shown in Fig. 1(e).

4. Order–disorder properties

The RLIII ordered structure has been chosen as the reference configuration at low temperature. We have successfully checked that the disordered equilibrium configurations reached by the MC simulations (described above) are independent on the initial configuration.

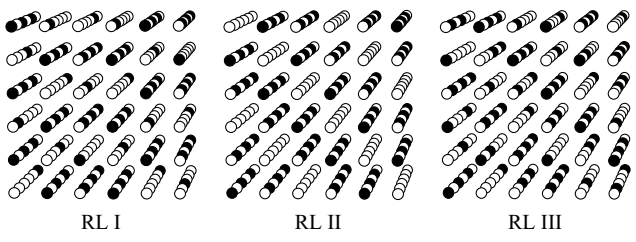

Fig. 2. Perspective view, along a <100> direction, of the B′ and B″ sublattices of the ordered RL structures given in Table 1. Full and open circles correspond to B^{II} and B^{V} cations, respectively. The sites of oxygen ions and cations A are not drawn.

4.1. Order–disorder transition

MC simulations have been performed at different temperatures. For low temperatures, exchanges are rare events. The energy is constant and the structure remains ordered. The associated heat capacity, C_V, computed as the energy fluctuations is thus equal to zero. Above a determined temperature that we define as a critical one, the exchanges take place frequently, the energy increases and C_V exhibits an abrupt variation corresponding to an order–disorder transition.

The values of the temperature are meaningless since the interactions model is purely coulombic (see Section 2). Nevertheless, the order–disorder critical temperature obtained, T_C, corresponds to a characteristic energy close to 0.29 e^2/a. To obtain an order of magnitude of the critical temperature value, we have to include the screening effect via the dielectric constant, ε. Using $a=0.405$ nm and $\varepsilon \sim 7$–12, T_C ranges from 1000 to 1700 K. Analysis of the structure along the equilibrium MC trajectory at T_C shows that the system periodically alternating between the ordered state RLIII and a disordered one. Moreover the RLIII hexagonal-axes changes and is oriented successively according to the four equivalent <111> directions (Fig. 3). On average, the probability so that the structure is ordered at this temperature is about 56%.

Fig. 4 shows that the Madelung constant decreases (i.e. an increase of the potential energy) as the temperature increases. The associated heat capacity (Fig. 4) presents a pronounced peak: C_V is divided by ~ 6 while T/T_C ranges from 1 to ~ 1.3. This is the signature of a phase transition that in this case

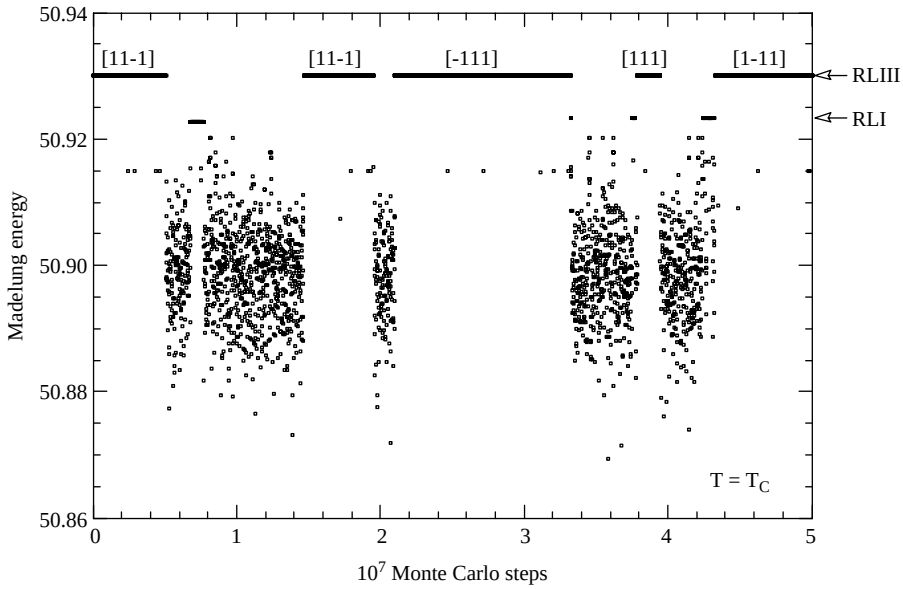

Fig. 3. Evolution of the Madelung energy during an equilibrium Monte Carlo trajectory at $T=T_C$. The system alternates between ordered RLIII or RLI structures and a disordered state. The hexagonal axes of RLIII are indicated.

corresponds to an order–disorder transition in the B′ sub-lattice. For higher temperatures, C_V decreases slowly and linearly with T/T_C. It is important to note that, although the melting point T_f of these compounds is about 1700 K [25] ($T_f/T_C<2$), calculations were carried out at temperatures higher than the experimental T_f in order to follow the evolution towards the randomly disordered state.

4.2. Order–disorder parameters

In order to characterise the disorder in the B′ sub-lattice, we chose to use short-range order parameters (SRO) as those defined by Cowley for metallic alloys [26]. The first ($i=1$) and second ($i=2$) neighbours SRO parameters, α_1 and α_2, respectively, are given by:

$$\alpha_i = 1 - \frac{P_i(B^{II})}{2/3} \quad (1)$$

where $P_i(B^{II})$ is the probability to find a B^{II} atom as i^{th} neighbour around a B^V atom, knowing that the atomic fraction of B^{II} atoms in the B′ sub-lattice is equal to 2/3. The first and second neighbour distances are equal to $\sqrt{2}a$ and $2a$, respectively. For randomly disordered configurations, $P_i(B^{II})$ tends to 2/3 and then α_i tends to zero.

For ordered configurations ($T<T_C$) of the 'random-layer' structure, Table 1 shows that RLII and RLIII have the same values for α_1 and α_2. These values are the low-temperature ones plotted in Fig. 5. The RLI configuration differs from the previous ones by a different value of α_2 and that corresponds to a slightly higher Madelung energy. For $T>T_C$, a local order remains and decreases slowly as the temperature increases. As the temperature increases the system tends towards the randomly disordered configuration. The second neighbour order vanishes whereas the first neighbour one does not.

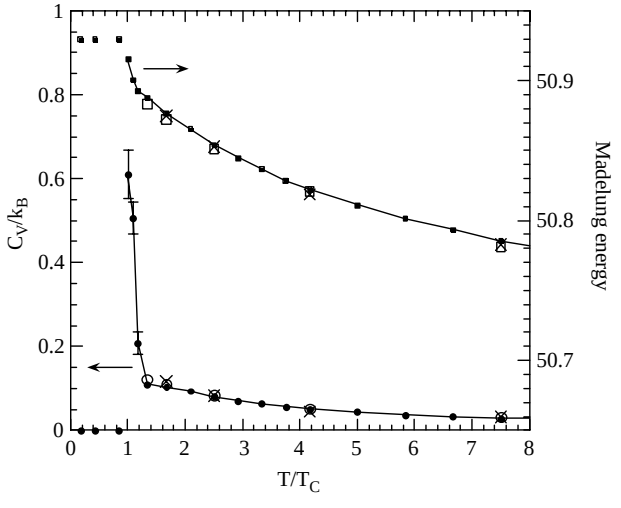

Fig. 4. Heat capacity at constant volume (circles) and Madelung energy (squares) plotted as a function of the temperature. The temperature is normalised to the critical temperature, T_C. For $T<T_C$, markers correspond to the ordered state at $T=0$ K. Full, open markers and crosses correspond to $6\times6\times6$, $12\times12\times12$ and $18\times18\times18$ cells, respectively. The error bars indicate the difficulty to calculate the heat capacity at T_C. k_B is the Boltzmann' constant.

4.3. Electric dipole moment

Considering that the exchange operate on two ions having different charges (+2 and +5), we can also characterise the thermal evolution of the system by the magnitude of the electric dipole moment computed for the volume of the $6\times6\times6$ box. Fig. 5 shows this evolution. In the ordered state, the moment is, as expected, equal to zero. At T_C, the moment increases abruptly to reach a value near 0.11 *e a* per unit cell (ABO_3) which corresponds to a polarisation of about 0.1 C m^{-2}. This quantity, due to the chemical disorder, has the same order of magnitude as the polarisation associated to the atomic shifts occurring in the ferroelectric phases [27]. We emphasise that

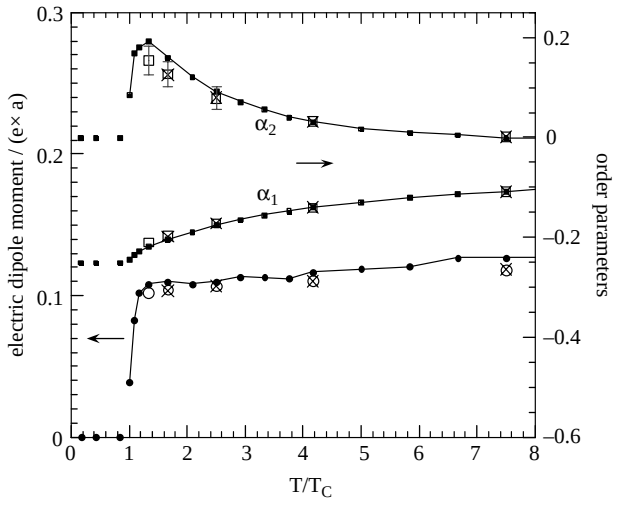

Fig. 5. Short-range order parameters (squares) and average magnitude of the electric dipole moment (circles) of the unit cell of 5 atoms, normalised by the electron charge and the lattice parameter ($e \times a$), plotted as a function of the temperature. α_1 and α_2 correspond to the first and second neighbours parameters, respectively. For the meaning of T_C, full, open markers and crosses see Fig. 4.

the latter contributes to the switchable polarisation of a given sample while the former does not. Its variation at higher temperatures is a very slight increase with increasing temperature. Therefore, this quantity cannot be used to characterise the disorder evolution as can be done using α_1 and α_2. It could be considered as a long-range order parameter. On the other hand, the lower value of the moment (0.05 *e a* per unit cell) around T_C is due to the fact that the system 'periodically' alternates between the ordered state RLIII and a disordered one (Fig. 3).

4.4. Size effect

For such a study of the structural order, we must check that the results obtained are not influenced by the limited size of the simulation box. This is the reason why calculations have been carried out on a larger system, namely a $12\times12\times12$ box. Since these calculations require too much CPU time, and especially close to T_C, only some temperatures have been checked. The high-temperature results are identical for both sizes, as shown in Figs. 4 and 5 (see points at $T/T_C > 4$) and slight discrepancies are observed for lower temperatures. In fact, the discrepancy increases as the temperature is closer to T_C. Concerning the Madelung energy, C_V and α_1 (Figs. 4 and 5), the agreement between the two box sizes is good. The results obtained with a $18\times18\times18$ system leads to the same conclusions.

Nevertheless, a more important discrepancy is observed for α_2 (Fig. 5). In this case, the size effect can be explained by comparing the second neighbour distance (2 *a*) to the half sizes of the three boxes: 3 *a*, 6 *a* and 9 *a*. The sampling is less efficient in the small box because we cannot 'find' two atoms with independent neighbours included in a sphere of radius 2*a*. In other words, the second neighbour distributions are correlated. In addition, the closeness of the α_2 values associated with the $12\times12\times12$ and $18\times18\times18$ boxes corroborates this explanation.

The electric dipole moment in the $12\times12\times12$ system has been computed over sub-systems of the same size as the $6\times6\times6$ system (see appendix for details). Therefore, the eight obtained values are averaged and reported in Fig. 5. We note that the values of the $12\times12\times12$ and $18\times18\times18$ systems undergo the same behaviour as the $6\times6\times6$ one.

In conclusion, the $6\times6\times6$ system provides satisfying results and no redhibitory size effect has been observed.

5. Discussion and conclusions

These results show that the B′ sub-lattice should not be a pure random mixture of ($B^{II}_{2/3}B^{V}_{1/3}$). In fact, the local order parameters at temperatures approaching T_f ($\sim 2\ T_C$) are far from being null (Fig. 5) as that is awaited if the B′-sites would be randomly occupied. At these temperatures, a local order remains and is characterised by a probability equal to 0.8 (instead of 0.67) to find a B^{II} atom around a B^{V} atom at the distance $\sqrt{2}a$. On the other hand, although the disorder is weak, the electric polarisation due to the chemical disorder, presents rather important values. The calculated value of the electric dipole moment for a $6\times6\times6$ box, corresponds to a polarisation of about 0.1 C m^{-2}. However, this disorder-induced local anisotropy is not consistent any more with the cubic Fm $\bar{3}m$ symmetry and suggests that relaxation is needed in the system; ions should be shifted from their centred positions due to the disorder-induced local electric field. Such ion displacements will thus contribute to a local polarisation of the system. Indeed, a polarisation fluctuation ranging from 0.05 to 0.25 C m^{-2} was measured in the temperature range 600–300 K in which the structure is assumed to be cubic with an average polarisation equal to zero [27]. This disorder-induced local anisotropy effect was used recently to explain the existence of the first-order Raman scattering [28] and the NMR line shapes [29] in PMN with average cubic symmetry.

These results about the local cations rearrangement in the Pb $B^{II}_{1/3}B^{V}_{2/3}O_3$ compounds should make it possible to look further into modelling, by taking into account the non-coulombic terms or by a full ab initio study in order to determine the real ferroelectric structure. Moreover, it is important to confirm in the future, the existence of the ordered structures RLI, II and III which will be probably used as basic structures for the first stage of calculations.

Acknowledgements

We acknowledge Gilbert Calvarin for fruitful discussions.

Appendix

We try to define an electric dipole moment $\vec{p}$ for a non-neutral charge distribution ($\vec{r}_i, q_i$). From the total positive and negative charges $Q^{(+)}$ and $Q^{(-)}$, we define 2 ΔQ as the total charge $Q^{(+)}+Q^{(-)}$ of the distribution and 2 Q as the difference

$Q^{(+)}-Q^{(-)}$. The total charge moment can be expressed as following

$$\sum_i q_i\vec{r}_i = Q^{(+)}\vec{r}^{(+)} + Q^{(-)}\vec{r}^{(-)}$$

$$\sum_i q_i\vec{r}_i = Q[\vec{r}^{(+)} - \vec{r}^{(-)}] + \Delta Q[\vec{r}^{(+)} + \vec{r}^{(-)}]$$

where $\vec{r}^{(+)}$ and $\vec{r}^{(-)}$are the charge-weighted averaged positions for positive and negative charges, respectively. We note that the quantity

$$\vec{p}_1 = \Delta Q[\vec{r}^{(+)} + \vec{r}^{(-)}]$$

corresponds to a monopolar charge. On the other hand the quantity

$$\vec{p} = Q[\vec{r}^{(+)} - \vec{r}^{(-)}]$$

corresponds to an electric dipole moment. One can note that in the case of a neutral charge distribution, $\vec{p}_1$ vanishes and the total charge moment corresponds to the electric dipole moment $\vec{p}$.

In our case of both the $12\times12\times12$ and $18\times18\times18$ systems, $\vec{p}$ has been computed over non-neutral sub-systems, of the same size as the $6\times6\times6$ system. For disordered structures the average value of ΔQ is about e.

References

[1] G.A. Smolenskii, A.I. Agranovskaya, Sov. Phys. Tech. Phys. 3 (1958) 1380.
[2] J. Kuwata, K. Uchino, S. Nomura, Jpn. J. Appl. Phys. 21 (1982) 1298.
[3] L.E. Cross, Ferroelectrics 76 (1987) 241.
[4] L.E. Cross, Ferroelectrics 151 (1994) 305.
[5] T. Mishima, H. Fujioka, S. Nagakari, K. Kamigaki, S. Nambu, Jpn. J. Appl. Phys. 36 (1997) 6141.
[6] N. Setter, L.E. Cross, J. Mater. Sci. 15 (1980) 2478.
[7] C.A. Randall, D.J. Barber, R.W. Whatmore, P. Groves, J. Mater. Sci. 21 (1986) 4456.
[8] C.G. Stenger, A.J. Burgraaf, Phys. Stat. Sol. (A) 61 (1980) 275.
[9] H.B. Krause, J.M. Cowley, J. Wheatley, Acta Cryst. A 35 (1979) 1015.
[10] P. Bonneau, P. Garnier, E. Husson, A. Morell, Mater. Res. Bull. 24 (1989) 201.
[11] D.M. Fanning, I.K. Robinson, X. Lu, D.A. Payne, J. Phys. Chem. Solids 61 (2000) 209.
[12] J. Chen, H.M. Chan, M.P. Harmer, J. Am. Ceram. Soc. 72 (1989) 593.
[13] C. Boulesteix, F. Varnier, A. Lebaria, E. Husson, J. Solid State Chem. 108 (1994) 141.
[14] L.A. Bursill, Hua Qian, JuLin Peng, X.D. Fan, Physica B 216 (1995) 1.
[15] Y. Yan, S.J. Pennycook, Z. Xu, D. Viehland, Appl. Phys. Lett. 72 (1998) 3145.
[16] P.K. Davies, M.A. Akbas, J. Phys. Chem. Solids 61 (2000) 159.
[17] W. Dmowski, M.K. Akbas, T. Egami, P.K. Davies, J. Phys. Chem. Solids 63 (2002) 15.
[18] L. Farbre, M. Valant, M.A. Akbas, P.K. Davies, J. Am. Ceram. Soc. 85 (2002) 2319.
[19] M. Akbas, P.K. Davies, J. Am. Soc. 81 (1998) 670.
[20] I. Qazi, I.M. Reaney, W.E. Lee, J. Eur. Ceram. Soc. 21 (2001) 2613.
[21] C.H. Lei, G. Van Tendeloo, S. Amelinckx, Phil. Mag. A 82 (2002) 349.
[22] L. Bellaiche, David Vanderbilt, Phys. Rev. Lett. 81 (1998) 1318.
[23] J. García, M. Meyer, M. Hayoun, Modelling Simul. Mater. Sci. Eng. 9 (2001) 81.
[24] D. Frenkel, B. Smit, Understanding Molecular Simulation, Academic Press, San Diego, 1996. p. 345.
[25] Y. Hosono, Y. Yamashita, H. Sakamoto, N. Ichinose, Jpn. J. Appl. Phys. 42 (2003) 5681.
[26] Y. Adda, J.M. Dupouy, J. Philibert, Y. Quéré, Eléments de métallurgie physique, INSTN-CEA Collection enseignement, Saclay, vol. 3, 1987 p. 626, Ch. 19.
[27] L.E. Cross, Ferroelectrics 76 (1987) 241.
[28] O. Svitelskiy, J. Toulouse, G. Yong, Z.G. Ye, Phys. Rev. B 68 (2003) 104107.
[29] R. Blinc, A. Gregorovic, B. Zalar, R. Pirc, V.V. Laguta, M.D. Glinchuk, Phys. Rev. B 63 (2001) 024104.